Structure and Properties of Polymethylsilsesquioxane Aerogels Synthesized with Surfactant *n*-Hexadecyltrimethylammonium Chloride

Gen HAYASE, Kazuyoshi KANAMORI,* Kazuki NAKANISHI

Department of Chemistry, Graduate School of Science, Kyoto University, Kitashirakawa, Sakyo-ku, Kyoto 606-8502, Japan

Corresponding author: Kazuyoshi KANAMORI, Dr. Eng.

Department of Chemistry, Graduate School of Science, Kyoto University, Kitashirakawa, Sakyo-ku, Kyoto 606-8502, Japan.

Tel/Fax: +81 75 753 7673, E-mail: kanamori@kuchem.kyoto-u.ac.jp

Abstract

Structure and physical properties of monolithic polymethylsilsesquioxane (PMSQ, $CH_3SiO_{1.5}$) aerogels have been systematically examined with varied starting compositions using a sol–gel system containing surfactant *n*-hexadecyltrimethylammonium chloride (CTAC). The precursor methyltrimethoxysilane (MTMS) undergoes hydrolysis and polycondensation under an acid-base

two-step reaction to obtain uniform gels as a one-pot reaction. To compare the samples, each factor of starting composition, such as amount of CTAC, concentration of aqueous acetic acid solution, volume of solvent and amount of urea, is independently varied. With appropriate concentrations of surfactant CTAC, the aerogels with high light transmittance (at 550 nm) are obtained, owing to the effective suppression of macroscopic phase separation. Acid-base catalysts, acetic acid and urea also impose significant effects on the properties of obtained aerogels including their molecular-level structures. The aerogel with 91 % of light transmittance was obtained under an optimized condition. The lowest density of the PMSQ aerogel in this system reaches 0.045 $g \cdot cm^{-3}$.

Keywords

Polymethylsilsesquioxane; Sol–gel; Aerogels; Organic-inorganic hybrid

1. Introduction

Aerogels are prepared with various chemical compositions ranging from inorganic oxides such as silica and alumina, to organic cross-linked polymers such as resorcinol-formaldehyde (RF) resins [1-3]. Typical high-quality silica aerogels, which are generally prepared by the sol-gel process, possess high porosity (> 90 %) and small pore size (~50 nm) with the porous texture consisting of aggregates of silica nanoparticles (~10 nm). Owing to these structural features, a number of excellent properties are attained; high transparency, low refractive index, low thermal conductivity, and low dielectric constant. In particular, applications to (transparent) thermal insulators [4-6], catalyst supports [7,8], supercapacitors [9,10], and low-*k* materials [11] are widely concerned and much effort is made to fabricate aerogels with low-cost and efficient mass production processes. However, aerogels are inherently brittle due to the high porosity and to the weak linkage of the aggregated particles. To keep the delicate pore structure intact during the removal of solvent from the precursor wet gels, supercritical drying instead of simple evaporative drying is required, in which high pressure (and high temperature) is needed. This fatal drawback keeps aerogels away from the extended applications.

To improve the mechanical properties, much effort has been paid so far. Some researchers investigated the effect of extended aging in water, monomer solution, and mother solvent [12,13] to dry wet gels in milder (*i.e.* subcritical) conditions or even under ambient pressure and temperature. During the aging process, small primary particles with high positive curvature preferentially dissolve and

re-precipitate onto the “neck” portion with high negative curvature in-between contacting particles. The resultant skeletal structure contains the smoothed linkage of particles, which increases the stiffness and strength of the original gel. Aging in monomer solution drastically enhances the mechanical properties by incorporating monomers from the aging solution into the as-prepared gel networks to increase the cross-linking density. Hybridization with organo-functional silanes or organic polymers is another promising way to increase the mechanical durability of aerogels [14-21]. Although sacrificing the transparency due to macroscopic phase separation of hydrophobic networks, organic-inorganic hybrid aerogels prepared from methyltrimethoxysilane (MTMS) [17] and MTMS/dimethyldimethoxysilane (DMDMS) coprecursors [21] show unusual flexibility.

Simultaneously, we have demonstrated that a modified two-step sol-gel process containing urea and surfactant prevents the occurrence of macroscopic phase separation, and transparent organic-inorganic hybrid aerogels are obtained utilizing MTMS as a single precursor [22-27]. The resultant ideal gel network is represented as polymethylsilsesquioxane (PMSQ, $CH_3SiO_{1.5}$). Urea is hydrolyzed into ammonia and carbon dioxide at 60 °C after the hydrolysis of MTMS which is catalyzed by dilute acetic acid, accelerating condensation and promotes homogeneous gelation by raising solution pH. In order to thoroughly suppress phase separation, we used appropriate surfactants which effectively suppress phase separation by making the MTMS-derived condensates hydrophilic. In the case of nonionic surfactant, poly(ethylene oxide)-*block*-poly(propylene oxide)-*block*-poly(ethylene

oxide) (EO_{106}-PO_{70}-EO_{106}, Pluronic F127) [29], it was deduced that MTMS-derived condensates were made hydrophilic by adsorbing through hydrogen bonding between ether oxygen of F127 and silanol groups of MTMS condensates. When cationic *n*-hexadecyltrimethylammonium salt (bromide CTAB or chloride CTAC) is employed, the MTMS condensates are more strongly made hydrophilic by weakly interacting with the hydrophobic chain of CTAB or CTAC. The resultant aerogels showed an unusual "spring-back" behavior which contains the compression of aerogel without cracking and the following perfect recovery when unloaded. Successful drying of wet gels without utilizing supercritical drying was also reported [22]. Low-density and transparent xerogels with comparable properties to corresponding aerogels thus obtained are promising for various applications such as to thermal insulators due to their potential for low-cost productions.

In the present paper, we show the control of pore structures and properties by systematically altering the starting composition. In particular, effects of changing concentrations of surfactant, urea and solvent are investigated. To minimize the effect of drying, all the gels have been processed by supercritical drying. The pore structure of aerogels is observed by field emission electron microscopy (FE-SEM). Properties including bulk density, light transmittance and compressive mechanical properties are also studied. The comprehensive information on relationships between starting compositions and physical properties is highly important to understand and design the pore properties of PMSQ aerogels/xerogels.

2. Experimental

2.1. Chemicals

Acetic acid, distilled water, urea, methanol, and 2-propanol were purchased from Hayashi Pure Chemical Ind., Ltd. (Japan). Surfactant *n*-hexadecyltrimethylammonium chloride (CTAC) was from Tokyo Chemical Ind. Co., Ltd. (Japan). Methyltrimethoxysilane (MTMS) was obtained from Shin-Etsu Chemical Co., Ltd. (Japan). All reagents were used as received.

2.2. Synthesis Procedures

The sample notations are defined, for example, as C*w*A*x*-*y*U*z*, where *w*, *x*, *y* and *z* are weight of CTAC (in g), concentration of aqueous acetic acid (in mM), volume of aqueous acetic acid (in mL) and weight of urea (in g), respectively.

At the typical starting composition C0.4A5-10U3, 10 mL of 5 mM aqueous acetic acid, 0.40 g of surfactant CTAC and 3.0 g of urea were dissolved in a glass sample tube, and then 5 mL of MTMS was added with vigorous stirring. The molar ratio of this typical starting composition is MTMS:water:acetic acid:urea:CTAC = $1.0:1.6 \times 10:1.4 \times 10^{-3}:1.4:3.6 \times 10^{-2}$. The mixed solution was continuously stirred for 30 min at room temperature for acid-catalyzed hydrolysis, followed by base-catalyzed gelation and aging at 60 °C in a closed vessel for 4 d. The typical gelation time was

about 3 h. The wet gels thus obtained were soaked in water/methanol (volume ratio 1:1) once, then methanol twice and 2-propanol three times each at 8 h intervals to remove CTAC and other unreacted reagents. Alcogels obtained in this way were dried from supercritical carbon dioxide at 80 °C, 14.0 MPa for 10 h in a custom-built autoclave (Mitsubishi Materials Corp., Japan) to obtain aerogels.

2.3. Measurements

The pore structure was observed with an FE-SEM JSM-6700F (JEOL Ltd., Japan). Bulk density, ρ_b, was obtained by measuring the volume and weight of a carved gel. Porosity ε (%) was then determined as $\varepsilon = (1 - \rho_b/\rho_s) \times 100$, where ρ_s represents true density that was fixed to be 1.40 g·cm^{-3} determined for a typical MTMS-derived aerogel by helium pycnometry. For light transmittance measurements, a UV-VIS spectrometer V-670 (JASCO Corp., Japan) equipped with an integrating sphere ISN-723 was employed. Direct-hemispherical transmittance was recorded, and obtained transmittance data at 550 nm were normalized into those of 10 mm-thick samples using the Lambert-Beer equation. The normalized total transmittance is denoted as T.

To assess the molecular structure of obtained PMSQ networks, FTIR measurement was performed with IRAffinity-1 (Shimadzu Corp., Japan) using an attenuated total reflection (ATR) attachment. A total of 100 scans were recorded with a resolution of 4 cm^{-1}. All samples were dried in vacuum at 80 ºC for 1 d in advance of the measurement.

Mechanical properties of aerogels were measured by a material tester Autograph (Shimadzu Corp. Japan). Carved aerogels (typical length × width × height is 8 × 8 × 5 mm^3) were compressed using a load cell of 5 kN. The measurements were performed by compressing up to 50 % of its original height with a rate of 0.5 $mm \cdot s^{-1}$ and then decompressing back to 0 N at the same rate. Young's modulus has been calculated using the slope of stress-strain curves between 0.1 and 0.2 MPa stress.

3. Results and Discussion

3.1. Effects of CTAC

In many reaction conditions, MTMS does not form uniform gel networks in polar solvents, due to the high phase separation tendency resulted from the strong hydrophobicity of the methylsiloxane networks. To synthesize uniform monolithic aerogels, we have developed the method utilizing surfactant in starting compositions to suppress phase separation. In C*w*A5-10U3 system, we obtained transparent elastic aerogels with $w > 0.10$ g of CTAC (molar ratio [CTAC]/[MTMS] > 0.009), and relationships are presented between w and several properties as T, ρ_b and Young's modulus in Fig. 1. Light transmittance at 550 nm showed the maximum at $w = 0.40$ g with $T = 89$ % (sample shown in Fig. 2 (a)). Bulk density ρ_b of this aerogel was 0.138 $g \cdot cm^{-3}$ and porosity, ε, was calculated as 90 %. With increasing w, the light transmittance value T gradually decreased due to decreasing network homogeneity. Although monolithic aerogels can be obtained even with > 4.00 g of CTAC

([CTAC]/[MTMS] > 0.36), translucency was low. In the cases of other surfactants, for example Pluronic F127, there is the upper limit of the amount of surfactant in the starting composition to obtain a monolithic gel. It is suggested that the interaction between CTAC and the MSQ condensates is weaker, and interruption of polycondensation hardly occurs. The attractive interaction may be predominantly based on the weak hydrophobic interaction between alkyl chains of CTAC and hydrophobic condensates.

With varying the amount of CTAC, microstructures (Fig. 3) as well as the physical properties of aerogels were changed. In C*w*A5-10U3 system, these changes can be explained by dividing into 4 regions about the *w* value. (1) In $w < 0.10$ ([CTAC]/[MTMS] < 0.009), macroscopic phase separation occurred because the amount of CTAC molecules is not enough to suppress the strong hydrophobicity of PMSQ networks. The resultant coarse structure is shown in Fig. 3 (a). (2) In $0.10 < w < 0.60$ (0.009 < [CTAC]/[MTMS] < 0.054), the gel network became uniform because the moderate amount of CTAC effectively interacted with the hydrophobic networks and suppressed phase separation. At $w = 0.40$ (Fig. 3 (b)), the aerogel exhibited the highest light transmittance and lowest density, as mentioned above. (3) In $0.60 < w < 1.20$ (0.054 < [CTAC]/[MTMS] < 0.11), excess CTAC molecules weakly interfere the network formation and gels shrank more during the solvent exchange and supercritical drying, due to the lower crosslinking density and weaker connections between particles composing the gel skeleton. At $w = 0.80$ ([CTAC]/[MTMS] = 0.072), shrinkage reached a maximum in this system, and the resultant finer

structure is exhibited in Fig. 3 (c). Bulk density and Young's modulus became larger than those of the aerogels in the region (2) as can be confirmed in Fig. 1 (a) and (c). These factors show a good correlation because both of these factors are strongly influenced by the shrinkage during aging, solvent exchange, and drying; the more shrinkage leads to the increased bulk density and Young's modulus. (4) With further increasing *w*, the microstructure became coarser (Fig. 3 (d)), and accordingly the less shrinkage has been observed. The larger particles and their less homogeneous aggregations decreased *T* because of the enhanced Mie scattering as can be confirmed in Fig. 1 (b). The mechanism of particles growth and their aggregations may be caused by multiple factors, such as increased stability of condensates covered with CTAC molecules in the solution with an excess of CTAC, which retards the nucleation of colloidal particles.

3.2. Effects of Acetic Acid

In acidic conditions, alkoxysilanes including MTMS are efficiently and uniformly hydrolyzed. No hydrolysis occurred without acetic acid in the starting solutions investigated in this study. We obtained monolithic aerogels when the concentration of acetic acid aqueous solution was in the range of x = 1-300 mM. Fig. 4 shows the relationships between properties of aerogels and x (C0.4Ax-10U3 system). With $1 < x < 10$, there are no changes in these three properties, but with $x > 10$, T gradually decreased. With $x > 60$, ρ_b became higher but Young's modulus did not clearly change due to the

higher shrinkage, which is caused by the enhanced formation of cyclic/polyhedral species (at 1100 cm^{-1}) instead of linear and branched species (at 1025 cm^{-1} [28]) as evidenced in the FTIR spectra in Fig. 5. The cyclic/polyhedral species do not contribute to the strength of the gel network, and lead to the formation of inhomogeneous gel network due to increasing phase separation tendency (Fig. S1). These results conclude the optimal concentration range of acetic acid to synthesize transparent aerogel is 1-10 mM. In this range, obtained aerogels possess almost the same properties, though hydrolysis rates are different.

3.3. Effects of Urea

Although transparent PMSQ aerogel cannot be obtained under the one-step acidic condition due to the enhanced formation of cyclic/polyhedral species, the basic condition promotes polycondensation of MTMS monomers and oligomers into the branched network, which provides the good condition to obtain transparent aerogel monoliths with uniform networks. We used urea as a base-releasing agent; urea is hydrolyzed into NH_4OH and CO_2 and uniformly raises pH of the aqueous sol. Fig. 6 shows the pH curve of the solution with the typical starting composition C0.4A5-10U3 (but without MTMS) measured at 60 ºC. In C0.4A5-10U3 system, the gelation time was ~3 h, and pH of the solution at the time was ~6.~~9~~8. After gelation, pH continued to rise and finally reached 9.1 after 4 d.

With varied amount of urea, properties and pore structures of aerogels are clearly changed as

shown in Fig. 7 and Fig. S2. Monolithic gels could not be obtained with less than 0.50 g of urea. Without urea in the starting composition, the sol was stable even when acetic acid was sufficiently diluted, whereas a small amount of oil was separated after a few days. In C0.4A5-10U*z* system, *T* increased and ρ_b and Young's modulus decreased with increasing amount of urea, which promoted polycondensation into random networks before an enhanced formation of cyclic/polyhedral species in the acidic condition owing to the higher rate of pH increase and shorter gelation time. The obtained networks also become homogeneous in such condition. In the C0.4A5-10U1 sample, the porous structure is coarser than that of C0.4A5-10U3 (Fig. S2). Comparing z = 3 and 4 g, the obtained aerogels had almost the same properties because the networks became sufficiently uniform with such high amounts of urea. In $z > 4$, urea does not completely dissolve in the solution containing CTAC.

3.4. Effects of Solvent Volume

Water acts as the diluting solvent as well as reactant in hydrolysis in the present system. Properties as well as pore structures of aerogels are also affected by the volumetric ratio of 5 mM acetic acid aqueous solution (y mL) / MTMS volume (5 mL, yielding 2.3 g solid if stoichiometric conversion is assumed) as shown in Fig. 8 and Fig. S3. We synthesized lower density aerogels by increasing the ratio of 5 mM acetic acid aqueous solution while fixing the concentration of urea (*i.e.* the y to z ratio is fixed in 10 to 3). With increasing y, ρ_b drastically decreased from ~0.50 to ~0.050 g·cm^{-3} (Fig. 8 (a))

in all y ranges. The Young's modulus naturally decreased accordingly with the decrease of bulk density (i.e. the decrease of monomer concentration).

In $y < 20$, no syneresis and shrinkage was observed during gelation and aging processes. This phenomenon is uniquely observed on aerogels synthesized with *n*-hexadecyltrimethylammonium (CTA) halide salts (CTAC and bromide CTAB), but rarely in the conventional silica aerogels systems. The absence of shrinkage and syneresis during gelation and aging is attributed to the repulsion between the polar head groups on the surface of the network [29]. This fact shows that this starting compositional region is advantageous to form the low-density monoliths by avoiding shrinkage by syneresis. The highest T was recorded at $y = 14$ with the value of 91 % (Figs. 8 (b) and S3 (c)). With further increase in y, T gradually decreased due to the disordering of pore structure by the higher shrinkage, which is caused by the lower mechanical strength of wet gels as shown in Fig.8 (c). In this system, crack-free aerogels are obtained when $y < 100$. At $y = 100$ (C0.4A5-100U30, the microstructure shown in Fig. S3 (d)), ρ_b and ε showed minima with the values 0.045 $g \cdot cm^{-3}$ and 97 %, respectively. This gel shrank ~30 % of the original size during drying due to the low mechanical strength, and the dried aerogel became translucent (Fig. 1 (b)). In addition, the outer surface of these samples was easily collapsed on fingers by absorbing oil from the human skin, whereas aerogels can float on water for at least a month. In $100 < y < 150$, monolithic aerogels were obtained, but they had too many and large cracks to characterize physical properties. Gelation occurred even when $y = 1000$, but the alcogels are easily

collapsed during solvent exchange so that dried monoliths cannot be obtained.

With decreasing y from 10, ρ_b steeply increased, which can be predicted from the starting compositions. On the other hand, T was dramatically changed. In $4 < y < 6$, T became lower than 20 %, because viscosity of the sol increased by high concentration of CTAC and the microstructure became coarser due to the inhomogeneous networks formation governed by a slow diffusion. The coarse microstructure and aggregations of PMSQ particles are shown in the FE-SEM image (Fig. S3 (a) and (b)). In $y < 4$, aerogels became denser and T became higher than those of in $4 < y < 6$, due to the significant shrinkage and densification during the aging process.

In summary, the range in y = 8-18 mL is the good condition to obtain aerogels with high transparency and the uniform gel networks. Outside this range, features of aerogels such as uniform microstructure and high porosity are lost.

4. Conclusions

Transparent PMSQ aerogels have been successfully obtained from MTMS under the co-presence of surfactant CTAC in the starting composition to suppress phase separation. As a result of the systematic study in this system, various properties of the aerogels are found to be affected by the starting composition. With the varied amount of CTAC, the porous texture of the gel is changed. To successfully obtain monolithic PMSQ aerogels, at least 0.10 g of CTAC ([CTAC]/[MTMS] = 0.009)

should be included in the solution. At 0.40 g of CTAC ([CTAC]/[MTMS] = 0.036), the obtained gel has the highest light transmittance, but decreases with increasing amount of CTAC. Density and Young's modulus are strongly correlated because both of these properties depend on the structure and strength of the gel networks. Concentrations of acid and base catalysts affect the molecular-level network and porous texture of the gels. With diluted acetic acid and increased amount of urea, we can obtain aerogels with high light transmittance and low density. With increasing the ratio of solvent volume to MTMS, density becomes lower and higher shrinkage occurred during gelation, solvent exchange and drying. The minimum density of PMSQ aerogels obtained without cracks is 0.045 $g \cdot cm^{-3}$, while light transmittance is partially sacrificed.

Acknowledgement

The present work was supported by Advanced Low Carbon Technology Research and Development Program (ALCA) from Japan Science and Technology Agency (JST). Also acknowledged is the Global COE Program ‘‘International Center for Integrated Research and Advanced Education in Materials Science’’ (No. B-09) of the MEXT, Japan, administrated by the Japan Society for the Promotion of Science (JSPS).

Supporting Information Available.

Additional FE-SEM images of the aerogel samples.

References

[1] J. Fricke, T. Tillotson, Thin Solid Films 297 (1997) 212-223.

[2] N. Hüsing, U. Schubert, Angew. Chem. Int. Ed. 37 (1998) 22-45.

[3] A. C. Pierre, G. M. Pajonk, Chem. Rev. 102 (2002) 4243-4265.

[4] K. Duer, S. Svendsen, Sol. Energy 63 (1998) 259-267.

[5] K. I. Jensen, J. M. Schultz and F. H. Kristiansen, J. Non-Cryst. Solids 350 (2004) 351-357.

[6] M. Reim, W. Körner, J. Manara, S. Korder, M. Arduini-Schuster, H.-P. Ebert, J. Fricke, Sol. Energy 79 (2005) 131-139.

[7] G. M. Pajonk, Appl. Catal. 72 (1991) 217-266.

[8] C. Moreno-Castilla, F. J. Maldonado-Hódar, Carbon 43 (2005) 455-465.

[9] R. Saliger, U. Fischer, C. Herta, J. Fricke, J. Non-Cryst. Solids 225 (1998) 81-85.

[10] E. Frackowiak, F. Béguin, Carbon 39 (2001) 937-950.

[11] W. Volksen, R. D. Miller, G. Dubois, Chem. Rev. 110 (2010) 56-110.

[12] A. Rigacci, M.-A. Einarsrud, E. Nilsen, R. Pirard, F. Ehrburger-Dolle, B. Chevalier, J. Non-Cryst. Solids 350 (2004) 196-201.

[13] R. A. Strøm, Y. Masmoudi, A. Rigacci, G. Petermann, L. Gullberg, B. Chevalier, M.-A. Einarsrud,

J. Sol-Gel Sci. Technol. 41 (2007) 291-298.

[14] B. M. Novak, D. Auerbach, C. Verrier, Chem. Mater. 6 (1994) 282-286.

[15] N. Hüsing, U. Schubert, J. Sol-Gel Sci. Technol. 8 (1997) 807-812.

[16] H. El Rassy, P. Buisson, B. Bouali, A. Perrard, A. C. Pierre, Langmuir 19 (2003) 358-363.

[17] A. Venkateswara Rao, S. D. Bhagat, H. Hirashima, G. M. Pajonk, J. Colloid Interface Sci. 300 (2006) 279-285.

[18] N. Leventis, Acc. Chem. Res. 40 (2007) 874-884.

[19] A. Fidalgo, J. P. S. Farinha, J. M. G. Martinho, M. E. Rosa, L. M. Ilharco, Chem. Mater. 19 (2007) 2603-2609.

[20] T.-Y. Wei, S.-Y. Lu, Y.-C. Chang, J. Phys. Chem. B 112 (2008) 11881-11886.

[21] G. Hayase, K. Kanamori, K. Nakanishi, J. Mater. Chem. J. Mater. Chem. 21 (2011) 17077-17079.

[22] K. Kanamori, M. Aizawa, K. Nakanishi, T. Hanada, Adv. Mater. 19 (2007) 1589-1593.

[23] K. Kanamori, M. Aizawa, K. Nakanishi, T. Hanada, J. Sol-Gel Sci. Technol. 48 (2008) 172-181.

[24] K. Kanamori, K. Nakanishi, T. Hanada, J. Ceram. Soc. Jpn. 117 (2009) 1333-1338.

[25] K. Kanamori, K. Nakanishi, Chem. Soc. Rev. 40 (2011) 754-770.

[26] K. Kanamori, J. Ceram. Soc. Jpn. 119 (2011) 16-22.

[27] K. Kanamori, Y. Kodera, G. Hayase, K. Nakanishi, T. Hanada, J. Colloid Interface Sci. 357 (2011) 336-344.

[28] H. Dong, J. D. Brennan, Chem. Mater. 18, (2006) 4176-4182.

[29] M. Meyer, A. Fischer, H. Hoffmann, J. Phys. Chem. B, 106, (2002) 1528-1533.

Figure captions

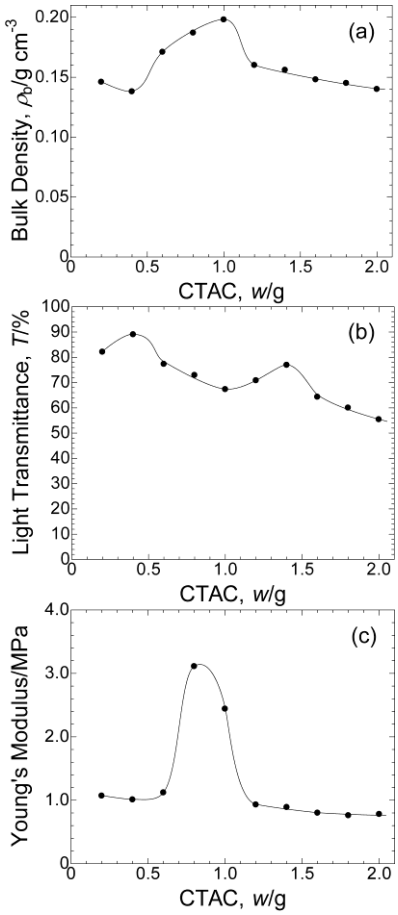

Fig. 1 Physical properties of aerogels derived with varied amount of CTAC (C*w*A5-10U3 system); (a) bulk density, ρ_b, (b) light transmittance at 550 nm^{-1}, T and (c) Young's modulus.

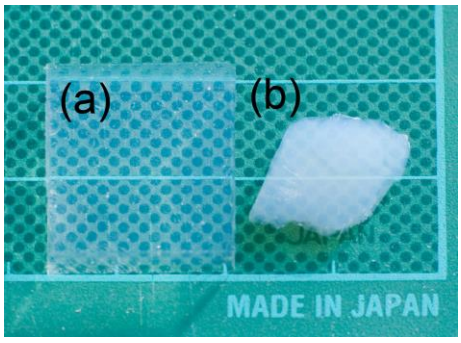

Fig. 2 Digital camera images of the obtained aerogels; (a) C0.4A5-10U3 and (b) C0.4A5-100U30.

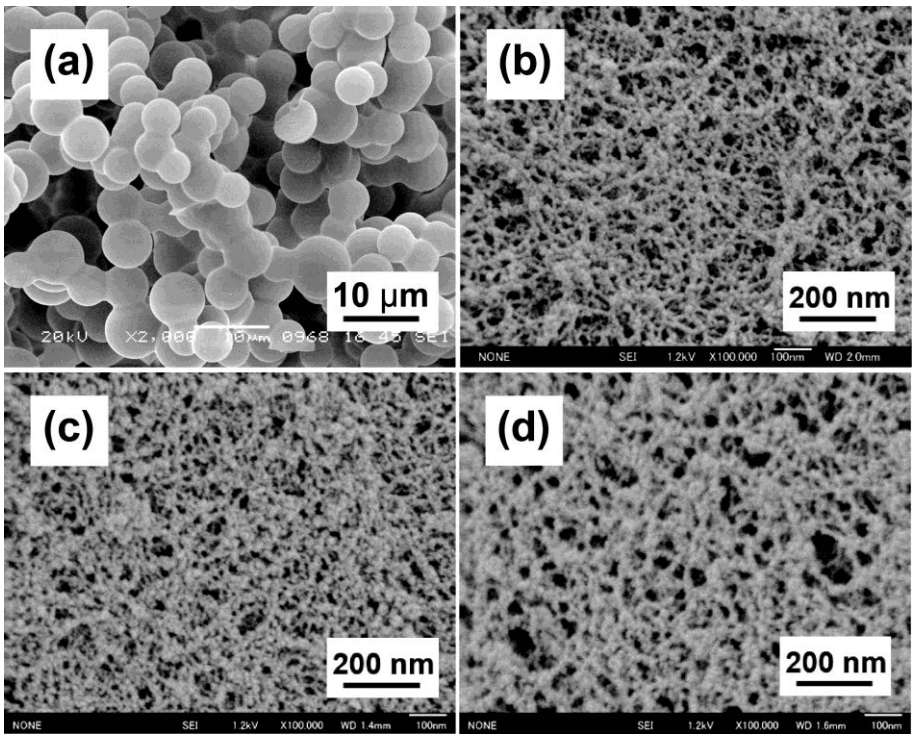

Fig. 3 SEM images of aerogels derived with varied amount of CTAC (C*w*A5-10U3 system); (a) *w* = 0 g, (b) 0.4 g, (c) 0.8 g and (d) 2.0 g.

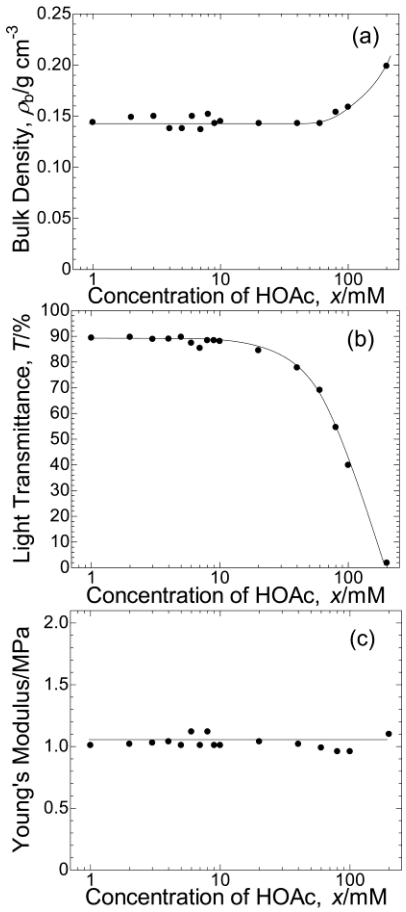

Fig. 4 Physical properties of aerogels derived with varied concentration of acetic acid aqueous solution (C0.4Ax-10U3 system); (a) bulk density, ρ_b, (b) light transmittance at 550 nm^{-1}, T and (c) Young's modulus.

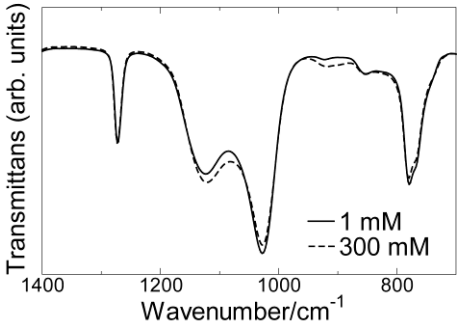

Fig. 5 FTIR spectra of aerogels derived with varied concentration of acetic acid aqueous solution (C0.4Ax-10U3 system); (a) 1 mM and (b) 300 mM.

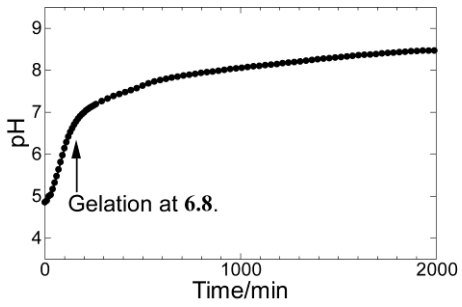

Fig. 6 Change in pH of the solvent with the typical starting composition C0.4A5-10U3 without MTMS at 60 °C.

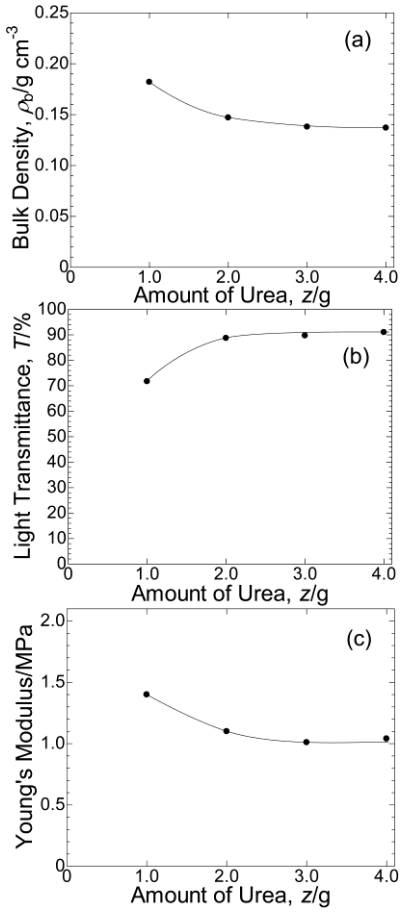

Fig. 7 Physical properties of aerogels derived with varied amount of urea, z (C0.4A5-10Uz system); (a) bulk density, ρ_b, (b) light transmittance at 550 nm^{-1}, T and (c) Young's modulus.

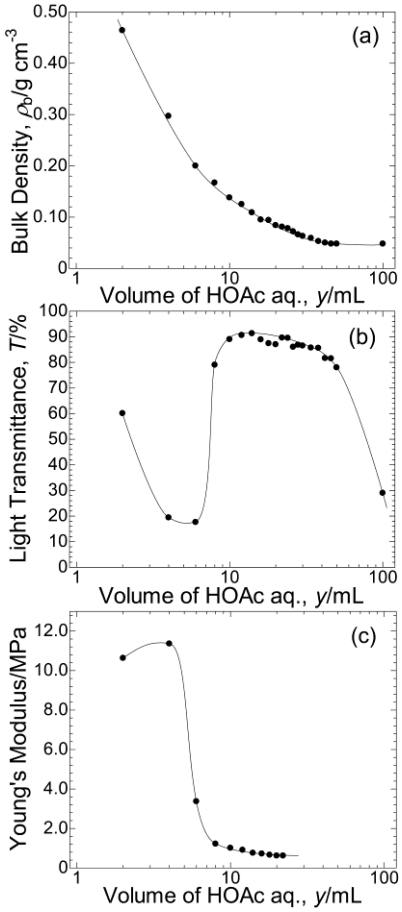

Fig. 8 Physical properties of aerogels derived with varied volume of solvent (C0.4A5-*y*U*z* system, with keeping *y*:*z* = 10:3); (a) bulk density, ρ_b, (b) light transmittance at 550 nm^{-1}, *T* and (c) Young's modulus.